Journal of Luminescence 153 (2014) 140–143

Contents lists available at ScienceDirect

Journal of Luminescence

journal homepage: www.elsevier.com/locate/jlumin

Synthesis and cathodoluminescence characterization of $ZrO_2:Er^{3+}$ films

A. Martínez-Hernández [a], J. Guzmán-Mendoza [a], T. Rivera-Montalvo [a,*], D. Sánchez-Guzmán [a], J.C. Guzmán-Olguín [a], M. García-Hipólito [b], C. Falcony [c]

[a] Centro de Investigación en Ciencia Aplicada y Tecnología Avanzada del Instituto Politécnico Nacional, Unidad Legaria, Av. Legaria 694, 11500 México, D. F., Mexico
[b] Instituto de Investigaciones en Materiales, Universidad Nacional Autónoma de México, Circuito Exterior, Cd. Universitaria, 04510 México, D. F., Mexico
[c] Centro de Investigación y de Estudios Avanzados del Instituto Politécnico Nacional, Apartado Postal 14-740, 07000 México, D.F., México

ARTICLE INFO

Article history:
Received 23 December 2013
Received in revised form
25 February 2014
Accepted 5 March 2014
Available online 14 March 2014

Keywords:
$ZrO_2:Er^{3+}$ films
Spray pyrolysis method
Cathodoluminescence
Metal oxides

ABSTRACT

Trivalent erbium doped zirconium oxide films were deposited by the ultrasonic spray pyrolysis technique. Films were deposited using zirconium tetrachloride octahydrate ($ZrCl_4O \cdot 8H_2O$) and erbium nitrate hexahydrate ($(NO_3)_3Er \cdot 6H_2O$) as precursors and deionized water as solvent. The dopant concentrations in the spray solution were 1, 3, 5, 10 and 15 at% in ratio to zirconium content. The films were deposited on corning glass substrates at different temperatures from 400 up to 550 °C. Films deposited at temperatures lower than 400 °C were amorphous, however, as substrate temperatures are increased, the ZrO_2 films presented a better crystallinity and showed a tetragonal phase. Cathodoluminescence (CL) emission spectra showed bands centred at 524, 544 and 655 nm associated with the electronic transition of Er^{3+}.

1. Introduction

In the last decade zirconium oxide (ZrO_2) has been widely studied for its physical and chemical features such as: high crystallographic density (5.7 g/cm^3), high fusion point (2715 °C), wide energy gap ($Eg=5.8$ eV), low phonon frequency, good thermal and chemical stability [1–4]. ZrO_2 is used as an additive to enhance the oxygen storage capacity (OSC) of the CeO_2 making it an efficient OSC material [5]. These characteristics make this material a potential candidate for multiple applications such as: electronic devices, wave of guide and dosimetric devices [6–8]. When this oxide is deposited as films it has a relatively high refractive index ($n=2.13$). ZrO_2 combined with silicon is suggested as a Metal-Oxide-Semiconductor (MOS) structure to replace silicon oxide, which has been widely used in microelectronics applications [9–11].

Zirconium oxide has been used as luminescent matrix of rare earth and transition metals. When it is activated with trivalent rare earth ions, it achieves remarkable photo and cathodoluminescent characteristics [12–15]. At the present time, zirconium oxide films have been deposited by several techniques such as: Chemical Vapour Deposition (CVD), Sol–Gel (SG) [16,17], Atomic Layer Deposition (ALD), Photochemical Metal Organic Deposition (PMOD) [4], and Ultrasonic Spray Pyrolysis (USP) [10]. The USP technique is an adequate technique to prepare films of many materials, mainly oxides, sulphides, and selenides. The UPS synthesis technique has resulted as versatile due its reactive organic and inorganic salts such as: chlorides, nitrates, acetates, acetylacetonates, ethoxides and butoxides dissolved on deionized water, ethanol or organic solvents [18]. The USP technique has many advantages over other synthesis methods: low cost, high deposition rates, easy to operate and capability to carry out deposition on large areas. In this paper the synthesis and cathodoluminescence characterization of $ZrO_2:Er^{3+}$ films deposited by ultrasonic spray pyrolysis technique are reported.

2. Experimental details

The ZrO_2 films were obtained using the Ultrasonic Spray Pyrolysis (USP) technique. The USP technique consists of a spray of precursor solution and it is directed onto the corning glass substrate which is previously heated, where the pyrolysis reaction is performed. Solutions of $ZrCl_4O \cdot 8H_2O$ from Alfa-Aesar with 99.99% degree of purity and $(NO_3)_3Er \cdot 6H_2O$ with 99% degree of purity were used as precursors, and deionized water as solvent. The spray solution concentration was 0.05 M and the substrate

* Corresponding author.
E-mail address: trivera@ipn.mx (T. Rivera-Montalvo).

http://dx.doi.org/10.1016/j.jlumin.2014.03.013
0022-2313/

temperatures were in the range of 400–550 °C with a flow rate of 10 L/min of the carrier gas (dry air). The deposition time was 5 min for all the samples in order to obtain films with almost the same thickness. In the erbium doped zirconium dioxide films, solutions at 1, 3, 5, 10 and 15 at% of erbium in relation to zirconium were used. The surface morphology and elementary composition were analyzed by Energy Dispersive X-ray Spectroscopy (EDS) using a Jeol Scanning Electron Microscopy (SEM) model LV6300 with an Oxford, INCA Energy+, Si–Li, X-ray detector. Crystalline structure of ZrO_2 films was determined using X-Ray Diffraction (XRD) technique in a SIEMENS D-500 diffractometer ($\lambda = 1.542$ °, CuK_α). The scan step was 0.02° using a counting time of 207.6 s. The range of 2θ was from 5 to 80. Cathodoluminescence measurements were carried out on a Luminoscope model ELM-2, Relion Co. with a vacuum metallic chamber at pressure of 55 mTorr. The films were exposed to a cold cathode electron beam with an accelerating voltage range from 4 to 12 kV on 2 kV steps and current of 0.3 mA. The chamber was coupled to a spectrofluorimeter FluoroMax-P brand, Jobin Yvon Horiba, using an optic fiber to obtain CL spectra.

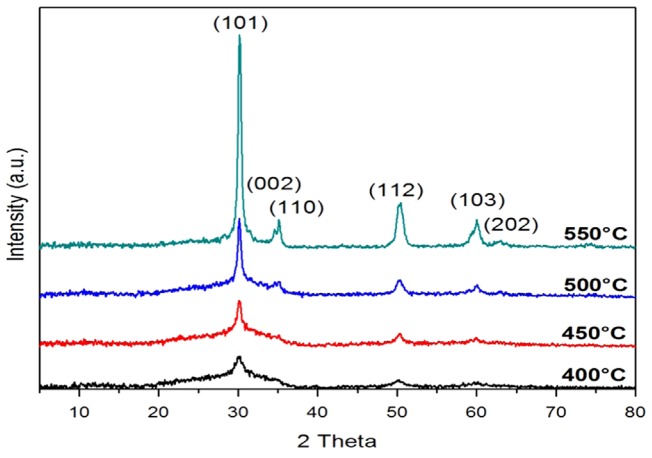

Fig. 1. XRD patterns of undoped ZrO_2 films deposited at different temperatures.

3. Results and discussion

The X-ray diffraction patterns of ZrO_2 films deposited at 400, 450, 500 and 550 °C are shown in Fig. 1. The films deposited at temperatures lower than 450 °C did not show well defined peaks; it is assumed that the deposited materials present an amorphous structure. Meanwhile, the X-ray diffraction patterns of ZrO_2 films deposited at 500 and 550 °C exhibited well defined peaks indicating a crystalline structure. In this figure as substrate temperature is increased better crystallization of the deposition material is observed; this is due to better distribution of thermal energy on the substrate surface. The stretching peaks indicate an increase of the crystal size as the temperature increases.

X-ray diffraction patterns of undoped films showed peaks that correspond to the tetragonal phase of ZrO_2 (according to 01-079-1764, ICSD 066783) with the most intense peak centred at $2\theta = 30.1°$ corresponding to crystallographic orientation (1 0 1). The crystal size was estimated using the Scherrer equation using the most intense peak [19]. Crystal size was determined to be 43 nm. In some times, X-ray diffraction patterns of ZrO_2 exhibit other peaks which correspond to a mixture of monoclinical and tetragonal phase. However, experimental results from this paper is not the case because the peaks exhibited are well defined and all peaks correspond to tetragonal phase. In Fig. 2, SEM micrographs of the surface morphology of undoped ZrO_2 films deposited at different substrate temperatures (e.g. 400, 450, 500 and 550 °C) are observed. In this figure the surface morphology of the films has a strong dependence on substrate temperature; films deposited at

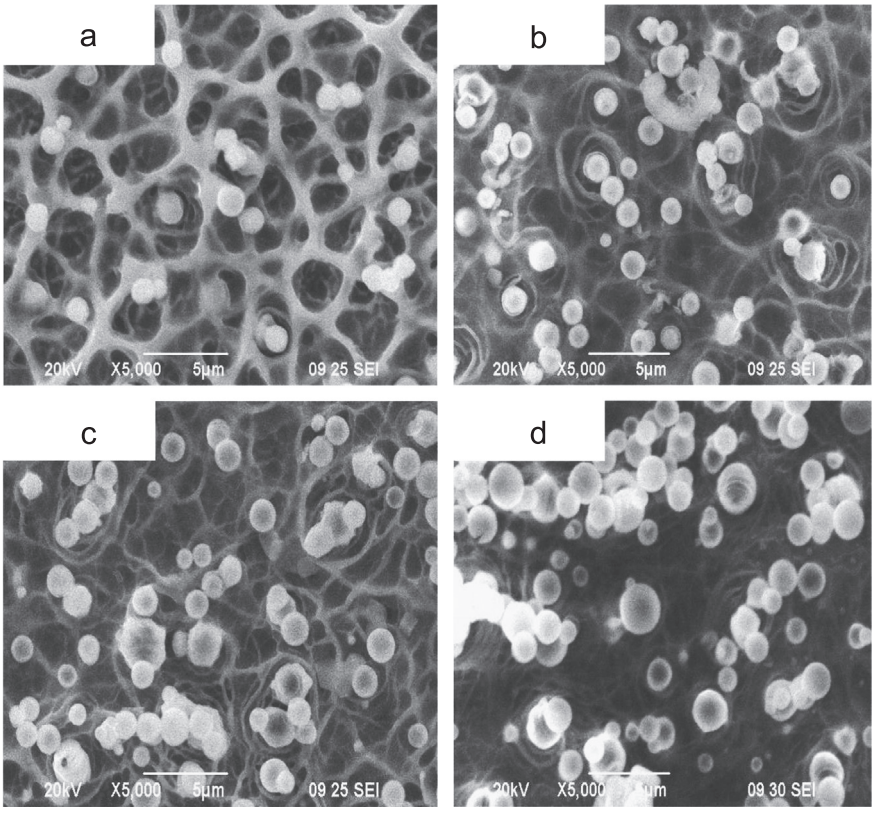

Fig. 2. SEM micrographs of undoped ZrO_2 films deposited at different temperatures.

temperatures between 400 and 450 °C present a porous open network surface formed by veins which may be a consequence of the impact of the precursors material in liquid phase over the hot substrate. As the deposition temperature is increased (500 °C) the network is closed and more compacted although rough surfaces are still observed. This microstructure could be attributed to higher substrate temperature effect. The thermal energy on the substrate is increased allowing a better pyrolysis reaction; at high temperatures deposition films showed a more compact surface with spherical particles which indicates that these particles have less contact with the substrate surface. However, as substrate temperature is increased up to 550 °C it may cause dissolvent evaporation and oxide formation on the proximities of the substrate surface. This reaction could provoke the accumulation of spherical particles that does not cover the substrate surface completely, as a consequence they have low adherence to the substrate. Homogenous morphology and high surface area on micrographs of film deposition at several substrate temperatures was seen which result in an advantage for some applications.

The relative concentration in atomic percentages of oxygen, zirconium, erbium and chlorine are shown in Fig. 3. This figure describes elementary composition of films deposited with 5 at% of erbium as a function of the deposition temperature determined by EDS technique. As it can be seen in the figure, the ratio of zirconium and oxygen almost is constant and this ratio is close to ideal stoichiometry. In this figure it is also observed that the chlorine content is decreased as substrate temperature is increased. As mentioned before, as deposition temperature is increased thermal energy on the substrate is increased which could then cause evaporation of chlorine.

The cathodoluminescent (CL) spectra of ZrO_2:Er^{3+} films deposited with 5 at% of erbium as a function of substrate temperature are shown in Fig. 4. The CL emission was obtained using an accelerator voltage of 8 kV. The highest CL emission was observed in the film deposited at 550 °C. This behaviour is attributed to higher crystalline quality, allowing better luminescence centre distribution, preventing their interaction and quenching effect.

Fig. 5 shows the CL emission spectra of ZrO_2:Er^{3+} films deposited at 550 °C with 5 at% of erbium ion as a function of accelerating voltage (V_a). Emission spectra of films were obtained by varying acceleration voltage from 4 to 12 kV on 2 kV steps. As voltage was increased CL emission intensity also increased; highest CL intensity was obtained when 12 kV was applied. This seems reasonable considering that when a higher voltage is applied electron penetration increases, in other words, a bigger material volume is excited, then more luminescent centres are activated. Increasing the luminescent centre concentration produces an increase of emission intensity.

Fig. 6 shows the CL spectra of the ZrO_2:Er^{3+} films deposited at 550 °C, excited with a voltage of 8 kV, as a function of the activator

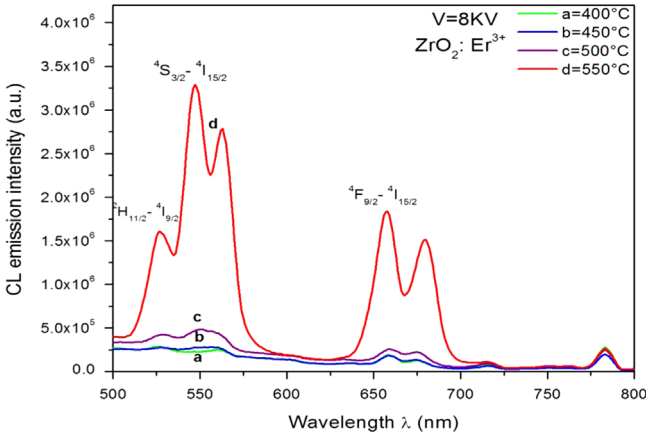

Fig. 4. CL emission spectra of ZrO_2:Er^{3+} (5%) films as a function of the substrate temperature.

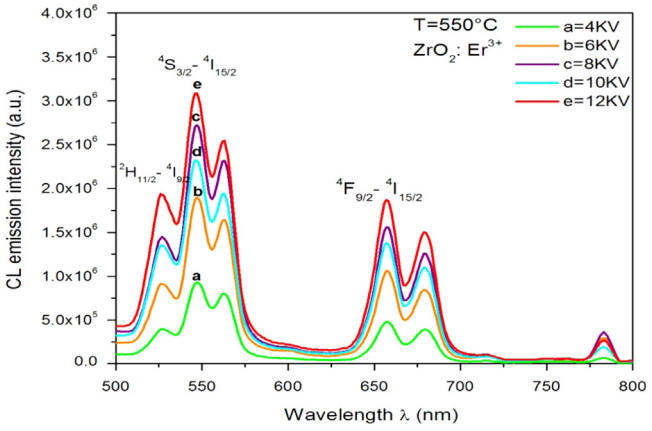

Fig. 5. CL emission spectra of ZrO_2:Er^{3+} (5%) films as a function of electron accelerating voltage.

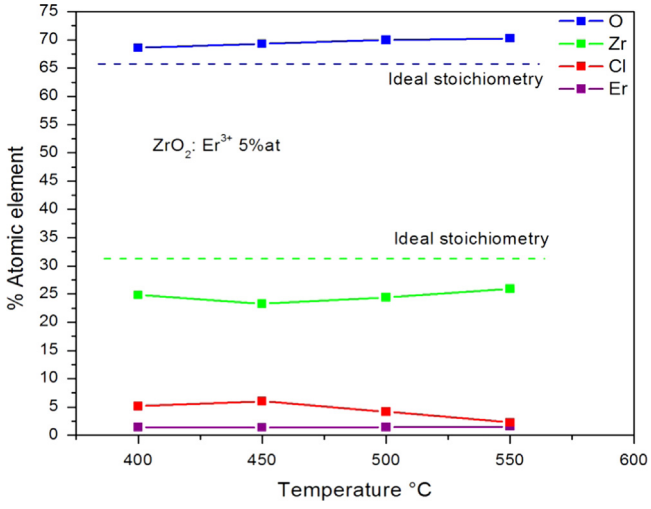

Fig. 3. Elementary composition of ZrO_2:Er^{3+} (5%) films as a function of the deposition temperature.

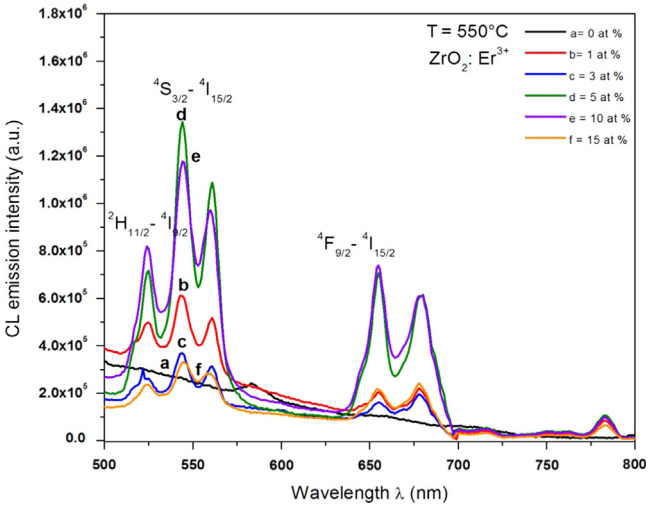

Fig. 6. CL emission spectra of ZrO_2:Er^{3+} films deposited at 550 °C as a function of dopant concentration.

ions (Er) concentration. As luminescence activator ion concentration increases CL intensity increases too until it reaches an optimal value of 5 at% of Er on initial solution. After this, ion impurity concentration an inhibition of CL intensity is observed (concentration quenching) [20].

As the dopant concentration is increased, the distance between the ions is reduced until a critical distance and after this energy transfer could be carried out between them; this effect produces less emission intensity. This phenomenon does not occur at lower ion concentrations because ions are not close enough for transfer of energy to occur.

4. Conclusions

In the present work undoped and erbium doped zirconium oxide films by ultrasonic spray pyrolysis were synthetized using zirconium tetrachloride and erbium nitrate as reactants. XRD patterns revealed crystalline structure of undoped zirconium oxide films that has a strong dependence on the substrate temperature. At low substrate temperatures the films were amorphous, as the deposition temperature was increased the structure of the films were mainly polycrystalline corresponding to tetragonal phase of the ZrO_2. SEM micrograph shows that the films were rough and continuous as the deposition temperature increased. The films deposited at high temperature show an ideal composition of zirconium oxide analyzed by EDS technique. The chlorine concentration was decreased as deposition temperature increased. The highest intensity of the CL emission was observed by the film deposited at 550 °C doped with 5 at% of erbium in relation to zirconium content. The CL spectra showed three peaks centred at 524, 544 and 655 nm that correspond to electronic transitions $^2H_{11/2}\rightarrow{}^4I_{15/2}$, $^2P_{3/2}\rightarrow{}^4I_{9/2}$, $^4S_{3/2}\rightarrow{}^4I_{15/2}$, and $^4F_{9/2}\rightarrow{}^4I_{15/2}$ characteristics of Er^{3+} ion. These transitions are in agreement with those reported in the literature [14].

Acknowledgements

This work was supported by the SIP-IPN Project numbers 20140528, 20140503 and 20130179.

References

[1] M. Morita, M. Baba, H. Fujiii, D. Rau, M. Yoshita, H. Akiyama, M. Herren, J. Lumin. 94–95 (2001) 191.
[2] J. Hoon, K. Sun, W. Jo, C. Jang-Hoon, J. Appl. Phys. 42 (2003) 2839.
[3] L. Lee-Jene, C. Tieh-Chiu, L. Meng-I, L. Yao-Kwang., Solid State Commun. 144 (2007) 181.
[4] G. Cabello, L. Lillo, C. Caro, G.E. Buono-Core, B. Chornik, M.A. Soto., J. Non-Cryst. Solids 354 (2008) 3919.
[5] J. Isasi, M. Pérez, J.F. Castillo, V. Correcher, I. Aldama, P. Arévalo, M.C. Carbajo., Mater. Chem. Phys. 136 (1) (2012) 160.
[6] T. Rivera Montalvo, L. Olvera Tenorio, J. Azorin Nieto, A. Campero Celis, C. Velazquez Ordoñez, R. Sosa Fonseca, J. Radiat. Eff. Defects Solids 159 (11–12) (2004) 645.
[7] T. Rivera, C. Furetta, J. Azorín, J. Mater. Sci. Forum 480–481 (2005) 373.
[8] T. Rivera, J. Azorín, M. Barrera, A.M. Soto, R. Sosa, C. Furetta, Radiat. Eff. Defects Solids 162 (7–8) (2007) 597.
[9] E. De la Rosa-Cruz, L.A. Díaz-Torres, P. Salas, V.M. Castaño., J. Phys. D: Appl. Phys. 34 (2001) L83.
[10] E. De la Rosa Cruz, L.A. Diaz-Torres, R.A. Rodríguez-Rojas, M.A. Meneses-Nava, O. Barbosa-García, Appl. Phys. Lett. 83 (24) (2003) 4903.
[11] X. Zhao, D. Vanderbilt., Phys. Rev. B 65 (2002) 075105.
[12] A. Patra, Chem. Phys. Lett. 387 (2004) 35.
[13] M. García Hipólito, R. Martínez, O. Alvarez-Fregoso, E. Martínez, C. Falcony, J. Lumin. 93 (2001) 9.
[14] E.W. Chase, R.T. Hepplewhite, D.C. Krupka, D. Kahng, J. Appl. Phys. 40 (6) (1969).
[15] J. Isasi-Marín, M. Pérez-Estébanez, C. Díaz-Guerra, J.F. Castillo, V. Correcher, M.R. Cuervo-Rodríguez, J. Phys. D: Appl. Phys. 42 (2009) 075418.
[16] L. Wen-Chao, D. Wu, L. Ai-Dong, L. Hui-Qing, Y. Feng, M. Nai-Ben, Appl. Surf. Sci. 191 (2002) 181.
[17] H. Zhang, X. Fu, S. Niu, Q. Xin, J. Non-Cryst. Solid 354 (2008) 1559.
[18] M. Langlet, J.C. Joubert., The pyrosol process or the pyrolysis of an ultrasonically generated aerosol, in: C.N.R. Rao (Ed.), Chemistry of Advanced Materials, Blackwell Science, Oxford, England, 1993, p. 55.
[19] B.D. Cullity, S.R. Stock, Elements of X-Ray Diffraction, third edition, Prentice Hall, New Jersey, USA, 2001.
[20] G. Blasé, B.C. Grabmaier, Luminescent Materials, Springer-Verlag, Berlin, Germany, 1994.